Examination of a Junction-Box Adhesion Test for Use in Photovoltaic Module Qualification

Preprint

David C. Miller and John H. Wohlgemuth

Presented at SPIE Optics + Photonics 2012
San Diego, California
August 12–16, 2012

NREL is a national laboratory of the U.S. Department of Energy, Office of Energy Efficiency & Renewable Energy, operated by the Alliance for Sustainable Energy, LLC.

Conference Paper
NREL/CP-5200-54185
August 2012

Contract No. DE-AC36-08GO28308

NOTICE

The submitted manuscript has been offered by an employee of the Alliance for Sustainable Energy, LLC (Alliance), a contractor of the US Government under Contract No. DE-AC36-08GO28308. Accordingly, the US Government and Alliance retain a nonexclusive royalty-free license to publish or reproduce the published form of this contribution, or allow others to do so, for US Government purposes.

This report was prepared as an account of work sponsored by an agency of the United States government. Neither the United States government nor any agency thereof, nor any of their employees, makes any warranty, express or implied, or assumes any legal liability or responsibility for the accuracy, completeness, or usefulness of any information, apparatus, product, or process disclosed, or represents that its use would not infringe privately owned rights. Reference herein to any specific commercial product, process, or service by trade name, trademark, manufacturer, or otherwise does not necessarily constitute or imply its endorsement, recommendation, or favoring by the United States government or any agency thereof. The views and opinions of authors expressed herein do not necessarily state or reflect those of the United States government or any agency thereof.

Available electronically at http://www.osti.gov/bridge

Available for a processing fee to U.S. Department of Energy
and its contractors, in paper, from:

U.S. Department of Energy
Office of Scientific and Technical Information
P.O. Box 62
Oak Ridge, TN 37831-0062
phone: 865.576.8401
fax: 865.576.5728
email: mailto:reports@adonis.osti.gov

Available for sale to the public, in paper, from:

U.S. Department of Commerce
National Technical Information Service
5285 Port Royal Road
Springfield, VA 22161
phone: 800.553.6847
fax: 703.605.6900
email: orders@ntis.fedworld.gov
online ordering: http://www.ntis.gov/help/ordermethods.aspx

Cover Photos: (left to right) PIX 16416, PIX 17423, PIX 16560, PIX 17613, PIX 17436, PIX 17721

Printed on paper containing at least 50% wastepaper, including 10% post consumer waste.

ABSTRACT

Engineering robust adhesion of the junction-box (j-box) is a hurdle typically encountered by photovoltaic (PV) module manufacturers during product development. There are historical incidences of adverse effects (*e.g.*, fires) caused when the j-box/adhesive/module system has failed in the field. The addition of a weight to the j-box during the "damp heat" IEC qualification test is proposed to verify the basic robustness of its adhesion system. The details of the proposed test will be described, in addition to the preliminary results obtained using representative materials and components. The described discovery experiments examine moisture-cured silicone, foam tape, and hot-melt adhesives used in conjunction with PET or glass module "substrates." To be able to interpret the results, a set of material-level characterizations was performed, including thermogravimetric analysis, differential scanning calorimetry, and dynamic mechanical analysis. PV j-boxes were adhered to a substrate, loaded with a prescribed weight, and then placed inside an environmental chamber (at 85°C, 85% relative humidity). Some systems did not remain attached through the discovery experiments. Observed failure modes include delamination (at the j-box/adhesive or adhesive/substrate interface) and phase change/creep. The results are discussed in the context of the application requirements, in addition to the plan for the formal experiment supporting the proposed modification to the qualification test.

Keywords: reliability, accelerated stress testing, polymers

1. INTRODUCTION

Component adhesion relies on the system of attachment, which includes the component itself, the adhesive(s), the surface preparation, and the substrate. Historically, the system of adhesion for junction boxes (j-boxes) has proven an essential product development task for photovoltaic (PV) module manufacturers. The possible consequences of failure in the field for the j-box include electrical arcing and subsequent initiation of fire. The detachment of the j-box (which interfaces between the module and outside world) also risks moisture ingress, subsequent corrosion, and the corresponding loss of performance. Possible failure mechanisms include: phase transformation, viscoelastic flow ("creep"), cohesive failure, and delamination [1]. Detachment of the j-box may also result from the degradation of the substrate (*e.g.*, delamination [2] or hydrolysis [3] of the backsheet, with the same consequences from failure).

The present module qualification tests [4],[5] only examine the adhesion of the j-box with the "robustness of termination" test [6]. In that test, a 40-newton load is applied for 10 seconds to the cables after the "ultraviolet (UV) preconditioning," "thermal cycling," and "humidity-freeze" sequence of tests. The robustness of termination test is performed with the cable in tension at room temperature. An additional test standard (Ref. [7], recently introduced to the International Electrotechnical Commission [IEC]) contains a section addressing retention of the j-box on the mounting surface. Here, a 40-N load is applied parallel to the module for 30 minutes (and then perpendicular to the module for 30 minutes) in a laboratory ambient environment. The retention test is performed after examining the mechanical strength of terminations and connections, knock-out inlets, cord anchoring, and j-box lid.

The module temperature can be estimated from the combined temperature, irradiance, and wind-speed data for a site using simple empirical models of the cell temperature [8],[9]. From these models, the maximum temperatures of 70°C and 90°C are expected for rack- and roof-mounted modules, respectively, each year based on the *average* weather conditions in the hottest desert locations in the world [10]. Furthermore, the temperatures of 85°C and 105°C are predicted for rack- and roof-mounted modules, respectively, based on the *30-year record* weather conditions in the same desert locations [10]. An even greater maximum temperature may be realized during the reverse-bias condition induced by partial shading, current mismatch, cracked cells, or interconnect failure. In this so-called "hot-spot" condition, the localized module temperature may exceed 150°C [11],[12], with resulting activation of the by-pass diodes and high temperature at the j-box. Other factors (*e.g.*, absorbed moisture) may also be present at elevated temperature, based on the meteorological field history.

To more vigorously interrogate the robustness of the j-box adhesion system, an amendment to the qualification test procedures has been proposed: hang a weight (vertically) from the junction box during the "damp-heat" test. The test would be performed at elevated temperature [85°C] for 1000 hours to emulate the real-world condition that may be encountered for some time over the expected module service life of 30 years. The test would be performed using an elevated moisture condition [85% relative humidity (RH)] at 85°C, a condition that is not expected to occur in a field-deployed module [13], but may be applied as an accelerated stress test to identify "infant mortality" failure

modes. The proposed amendment is cost-effective and time-effective, because it makes use of the existing qualification test protocol.

The goal of the study here is to provide a demonstration supporting the proposed amendment. Representative test specimens (adhesives including foam tapes, silicones, and hot-melts) have been evaluated in terms of their material characteristics, using thermogravimetric analysis (TGA), differential scanning calorimetry (DSC), and dynamic mechanical analysis (DMA). The proposed test procedure was performed using representative (polyethylene terepthalate [PET] or glass) substrates. The discovery experiments will be used to select the components (adhesives, substrates, and weights) that will be used in a formal demonstration, where specimens aged in a chamber will be compared to those aged in field locations.

2. EXPERIMENTAL

Images of the representative crystalline silicon (c-Si) and thin-film (TF) specimens are shown in Figure 1 and Figure 2. The specimens are photographed in a test fixture constructed of slotted fiberglass-reinforced channel (McMaster-Carr Supply Co.), used to hold them upright. The fixtures also include a deflector tray [labeled in Figure 1(b)], used to protect the second (lower) row of specimens in case specimens detach from the row above. TF (smaller and containing two rails to accommodate a single string of cells) and c-Si (larger and containing four rails to accommodate three cell strings) j-boxes were used in the separate experiments. J-boxes are typically constructed of Noryl (consisting of polyphenylene oxide and polystyrene) or Xyron (consisting of modified polyphenylene ether and polystyrene). The foam tapes examined (some obtained from different vendors) were made of acrylic, polyurethane (PU), or polyethylene (PE). A quick internet search identified PE tape as incompatible with PV substrate materials, making it an interesting candidate for evaluating the proposed test. All tapes had a closed cell construction, which limits moisture ingress. The foam tapes here are different from commercially available solid-core tape products. Several condensation (moisture-facilitated) cured silicones were examined, including those cured with acetoxy, oxime, or alkoxy curing chemistry. Because the acetoxy silicone produces acetic acid during curing, it is not recommended for PV (or other electronics). The known limited adhesion of acetoxy-cured silicone to polyethylene makes it useful for evaluating the proposed test. Low cost oxime silicone may not be used in many Western countries based on the volatile by-products. The alkoxy silicones examined here included Sn, Ti, and two-part-Sn catalyzed formulations. The hot-melts examined included ethylene-co-vinyl acetate (EVA), polyethylene/polyoctene copolymer (PO), and polyamide (PA). Although cross-linking hot-melts are available, the thermoplastic materials used here were intentionally chosen to validate the proposed test. A series of weights (obtained from JamFab Jigs and Custom Lures LLC, a fishing equipment manufacturer) was chosen for evaluation, including: 0, 0.5, 0.9, 1.4, 2.3, and 4.5 kg. Only one weight was attached to each j-box specimen.

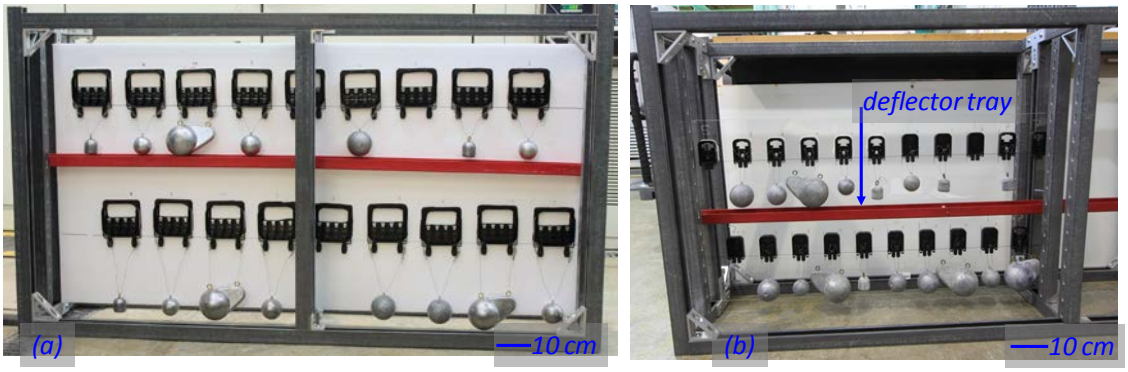

Figure 1: Representative (a) c-Si and (b) TF specimens, constructed for the discovery experiments. The deflector tray used to protect the second (lower) row of specimens is labeled in (b).

Details of the attachment of the j-boxes and the weights are shown in Figure 2 for the (a) c-Si [11.5 x 11.0cm] and (b) TF [7.0 x 5.2cm] specimens. The weights were secured using knots tied at the ends of 0.81-mm-diameter stainless-steel wire. The c-Si j-boxes were weighted using the tabs at the corners of the j-box. The predominant loading mode for all j-boxes was shear; however, some torque is possible for the c-Si boxes because the wire wrapped around the cable vias. The adhered surfaces of the c-Si j-boxes were smooth, with no groove or standoff features. For the TF j-boxes, the wire was secured through the cable gland sites (with the cable removed). J-box

cable glands are typically not designed to support a substantial sustained load; this prohibits applied loads at the cable gland sites in the proposed test. The adhered surfaces of the TF j-boxes were smooth, with no standoff features, but they included a ~2-mm-wide groove around the periphery (as typically used with a silicone bead). The lid was removed from all specimens through the discovery tests; therefore, temperature, oxygen and moisture could readily permeate the specimens.

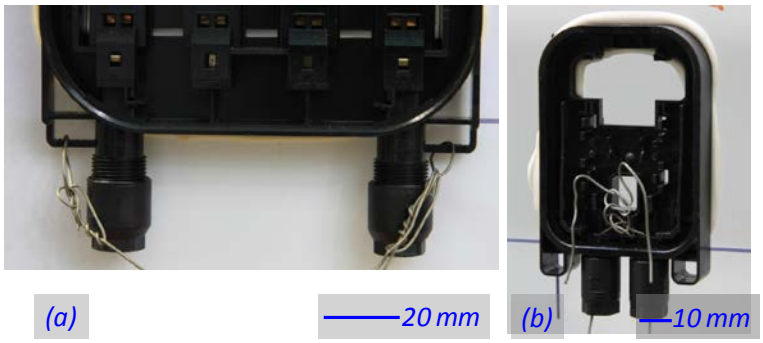

Figure 2: Details of the attachment (using steel wire) for the weights in the (a) c-Si and (b) TF specimens.

A series of material-level tests was performed on unaged adhesive specimens. The phase-transition temperatures were obtained using DSC (Q1000, TA Instruments – Waters LLC) and subsequently analyzed with the manufacturer's Universal Analysis 2000 software. The 2-Hz data were taken from the second of two consecutive cycles conducted from -180^0 to 200^{0}C at 10^{0}C•min^{-1} in a N_2 environment (purged at 50 mL•min^{-1}). TGA was performed using a Q500 (TA Instruments – Waters LLC). The instrument is capable of resolving mass loss to within 0.1 μg and temperature to within 1°C. A standard temperature ramp from the laboratory ambient to 800°C was used at the rate of 20°C•min^{-1}, with a data sampling rate of 0.5 Hz. The specimen chamber was continuously purged with reconstituted air (including both O_2 and N_2 gas) at 90 mL•min^{-1}. The mass loss and its derivatives {%, g•°C^{-1}, g•°C^{-2}} were calculated from the recorded data. DMA was performed using an Ares LS rheometer (TA Instruments – Waters LLC). Using nominally 12.6 mm x 30.5 mm (width x length) specimens, torsional data were obtained while heating from -65° to 150°C in a 1°C increment (step and hold). Specimen thickness varied from 1.0 to 3.0 mm, depending on the form factor, *e.g.*, molded or sheet material. A 2% oscillatory strain was applied (at the rates of 0.063, 0.63, 6.3, 63 Hz) along with a 20-g tensile load (to prevent specimen buckling) during DMA characterization.

Component-level specimens were assembled according to the manufacturer's guidelines. This included a cleaning of the glass substrate for TF, *e.g.*, buffing the tin-rich side of glass with pumice powder; followed by a detergent (Billco, Billco Manufacturing Inc.) rinse; followed by rinsing with deionized water (DI); followed by rinsing with isopropyl alcohol; followed by forced drying using clean dry air; followed by a site-specific silane primer (AP115, 3M Company). For c-Si, the PET backsheet was adhered to glass to mechanically support the c-Si specimens. A different primer (4298UV, 3M Company) was used on the PET and j-box to promote adhesion for all the tapes, which could be pressed in place (for ~5 seconds) using a 9.1 or 27.2 kg weight to ensure good wet-out. Because of their compliant and dissipative nature, a dwell time (on the order of 48 hours) may also improve the adhesion of foam tapes beyond their initial handling strength. The tape was cut out from the interior of the c-Si j-boxes (where the interconnects would feed through from the module interior). The tape was left in place for the TF j-boxes (which did not demonstrate good wet-out at the feed-through regions). A bead of adhesive was dispensed at the j-box periphery using a gun for the silicone and hot-melt specimens, *e.g.*, the inset of Figure 7 (b). Excess material was then squeezed underneath and to the sides of the j-boxes, when they were manually pressed into place, Figure 2(b). A larger bead (~4 mm) was used for the silicone (because of the geometry of the cartridges) than for the melts (~2 mm, because of the diameter of the heated nozzle of the Mini Squirt III gun [Nordson Benelux B.V.]). Additional details of the specimen attachment (including photographs of the compressed silicone or hot-melt bead obtained through the glass substrate) are provided in Ref. [14]. Specimens were photographed (40D, Canon Inc.), loaded into the "WITR" test chamber [SPX Corp. (Thermal Product Solutions Division)], exposed to 85°C/85% RH, and inspected periodically. The chamber had to be ramped down to the laboratory ambient condition from its operation at 85°C/85% RH.

3. RESULTS AND DISCUSSION

3.1 Material-level characterization (TGA and DSC)

The TGA results summarized in Table 1 include those of the material used for the body of the j-box. Representative data profiles are provided in Ref. [14]. The table includes the temperature at a specified mass loss (0.5, 5, or 50%) and the inflection-point temperature(s) (T_i, where $d^2m/dT^2 = 0$). In Table 1, m represents the specimen mass {g}, and T the temperature {°C}. In the table, no significant mass loss occurs below 200°C. The thermal decomposition characteristics of the tapes and melts are similar, with the silicones requiring an additional 100°C to decompose. The hydrocarbon materials (tapes and melts) typically demonstrated complete mass loss [14]; a significant weight (and corresponding char) remained for the silicones. The thermogravimetry of the condensation-cured silicones in Table 1 demonstrated similarities to the addition-cured silicones examined in Ref. [15], including: limited repeatability for specimens of the same formulation; irregular profiles (including instantaneous changes suggesting specimen motion); and the morphology and color of the remaining specimen char.

Table 1: Summary of the mass-loss characteristics for representative specimens, including the temperature at a specified mass loss (0.5, 5, or 50%) and the inflection-point temperature(s), *i.e.*, where $d^2m/dT^2 = 0$.

MATERIAL	DESCRIPTION or CURE SCHEME	$T_{0.5\%}$ mass loss {°C}	$T_{5\%}$ mass loss {°C}	$T_{50\%}$ mass loss {°C}	T_{i1}, max[dm/dT] {°C}	T_{i2}, max[dm/dT] {°C}	T_{i3}, max[dm/dT] {°C}
acrylic 1	foam tape	227	298	372	350	499	
acrylic 2	foam tape	220	314	379	379	533	
PE	foam tape	220	298	407	356	408	460
PU	foam tape	132	292	399	401	547	591
PA	thermoplastic hot melt	253	351	418	419	555	
PO	thermoplastic hot melt	228	289	367	380	537	
EVA	thermoplastic hot melt	190	261	385	415	547	
silicone	acetoxy (Sn catalyst)	220	421	505	510		
silicone	oxime (Sn)	241	390	520	527		
silicone	alkoxy (Ti)	133	387	718	411	564	749
silicone	alkoxy (2 part, Sn)	208	408	536	531	680	
Noryl	j-box body	293	429	468	454	614	

Regarding the interpretation of the TGA results, Table 1 is encouraging because it suggests that all of the adhesives can withstand temperatures ($T_{5\%}$) on the order of 150°C. (Consider that the decomposition temperature [at least 200°C in Table 1] may be decreased by ~50° when thermogravimetry is performed at slower rates than in Table 1.) The temperature of 150°C (or even somewhat hotter) is achievable locally at the cell and also at operating by-pass diode(s) in the j-box in a sustained hot-spot condition [11],[12]. Certain specimens (PU tape, EVA hot-melt, and alkoxy silicone) approach the suggested hot-spot temperature guideline for material decomposition ($T_{5\%}$). The minor mass loss at low temperatures for the silicone may come from the loss of a residual component, e.g., curing agent, and not decomposition. For these materials, a more rigorous verification—prolonged characterization at high temperature to verify integrity—makes sense. The j-box body is itself among the most thermally robust materials in Table 1 and Ref. [14].

The phase-transition temperatures are summarized in Table 2, which includes glass-transition temperature (T_α or T_g), melt-transition temperature(s) (T_m), and freeze-transition temperature(s) (T_f). Representative DSC data profiles are provided in Ref. [14]. The silicones are distinguished from the other materials because their phase transitions occur at temperatures significantly less than those typically encountered by fielded PV modules. All of the tapes have a T_g less than that typically encountered by fielded PV modules; the PE tape has melt transitions affecting a significant portion of the material, occurring at temperatures encountered in desert-deployed modules. All of the hot-melts have melt transitions at temperatures encountered in desert-deployed modules; the data for EVA identify that it has two such crystalline components.

A glass transition may signify propensity for creep, whereas a melt transition would be even more likely to indicate the onset of viscoelastic flow. The silicones would then readily creep, if they were not cross-linked by a curing

agent. A proper (and complete) cure is required to render the silicones as thermosets, preventing creep. The PE tape might creep in fielded modules, particularly in a prolonged hot-spot condition exceeding T_m. Table 2 suggests that all of the hot-melts might creep, because they have melt transitions occurring within the temperature range expected in desert-deployed modules. More extensive investigation would be advised for these latter materials, such as the proposed weighted j-box test. The j-box body material is verified using DSC (but not reported in Table 2) to have a glass transition at ~185 °C.

Table 2: Summary of the DSC results, including the glass-transition temperature (T_α or T_g), melt-transition temperature(s) (T_m), and freeze-transition temperature(s) (T_f).

TYPE	DESCRIPTION or CURING SCHEME	T_α=T_g {°C}	T_{f1} {°C}	T_{m1} {°C}	T_{f2} {°C}	T_{m2} {°C}	T_{f3} {°C}	T_{m3} {°C}
foam tape	acrylic 1	-43						
foam tape	acrylic 2	-56	86	99				
foam tape	polyethylene	-33	58	53	99	108		
foam tape	polyurethane	-26						
hot-melt	polyamide	-57	88	68				
hot-melt	polyolefin	-19	55	81		97		155
hot-melt	EVA	-3	20	75	65	99	87	
silicone	acetoxy (Sn catalyst)	-157	-69	-40				
silicone	oxime (Sn)	-155	-72	-40				
silicone	alkoxy (Ti)	-156	-78	-41				
silicone	alkoxy (2 part, Sn)	-149	-70	-42				

3.2 Results of "crystalline silicon" component-level specimens

The c-Si discovery experiment was conducted prior to the TF discovery experiment. Seven out of thirty-six c-Si j-box specimens failed the 1000 hour weight test in damp-heat. The first c-Si results concerned the PE tape, where all of the weighted specimens detached within 24 hours at 85°C/85% RH. The PE tape specimen with no weight attached remained adhered throughout the 1000 hour test. Representative images are shown in Figure 3, where cohesive failure of the tape's topmost adhesive layer is evident on the j-box [Figure 3 (bottom)]; the tape's core remained attached to the PET substrate [Figure 3 (top)]. The 2.3- and 4.5-kg weighted specimens demonstrated a tearing of the tape core [Figure 3 (top right)], whereas the lesser weighted specimens remained evenly adhered to the backsheet [Figure 3 (top left)].

Figure 3: Images of detached PE tape specimens (where all weighted specimens detached within 24 hours at 85°C/85%RH). The tape remained adhered to the PET substrate (image top) and not the j-box (image bottom).

The two acrylic tapes lost adhesion for the 4.5 kg weight between 6 and 7 days or between 7 and 14 days (respectively) at 85°C/85% RH when weighted with 4.5 kg. Images of the substrate and detached specimens are shown in Figure 4. In both cases, most of the tape remains adhered to the j-box [Figure 4 (bottom)] and not to the PET substrate [Figure 4 (top)]. For both tapes, the 4.5 kg weight is the only weight exceeding the manufacturer's design guideline [16].

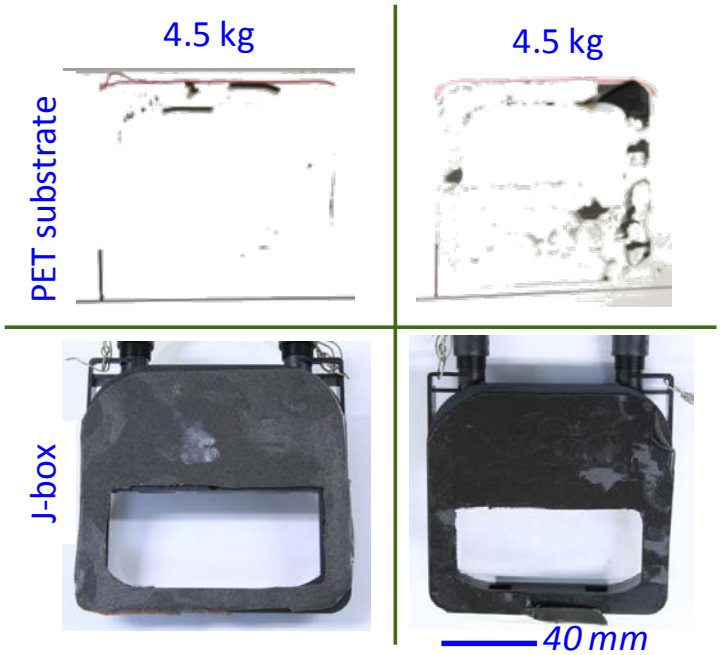

Figure 4: Images of the detached acrylic tape specimens (acrylic 1 and 2, occurring only when the applied load exceeded the manufacturer's design guideline). The tape remained adhered to the j-box (image bottom) and not to the PET substrate (image top).

The second acrylic tape deformed between 7 and 14 days or 14 and 21 days at 85°C/85% RH for the 2.3- and 1.4-kg weights, respectively. A representative image of these specimens is shown in Figure 5, where an irregular-shaped deformed region is circled at the top of the figure. These j-boxes remained adhered through the test and moved less than a millimeter relative to the location marked on the substrate prior to damp-heat exposure. The elongation in Figure 5 is therefore consistent with the manufacturer's intended dissipative behavior for the material. The behavior observed here during the c-Si test was not observed during the TF test for the same material. This implies that features of the "crystalline silicon" j-box design (e.g., the asymmetric geometry with the tape cutout at the top) may be specifically affecting the result. The first acrylic tape did not demonstrate the elongation shown in Figure 5.

Figure 5: Representative image of the deformed second acrylic tape, where one of the tape formulations was deformed for the 1.4- and 2.3-kg weights. These specimens did not elongate more than 1 mm and remained adhered through the damp-heat test.

None the tapes in the c-Si tests demonstrated evidence of creep. The torn appearance of the specimens in Figure 3 (top right) and Figure 4 (bottom left) may indicate a mixed-mode failure (where shear and bending were both present during the detachment). The materials examined are therefore limited by their adhesive characteristics. This implies the criticality of surface preparation for these materials, including proper cleaning, use of a primer, or plasma surface modification [17]. In the latter case, some removal of organic contamination is achieved in addition to carboxyl and carbonyl surface functionalization [17].

The potential issue of detachment identifies the need to use a system of compatible materials, including the j-box, adhesive, and substrate. Ultimately, there will be some upper limit to the adhesion (or cohesion of an adhesive layer as in Figure 3) that may be achieved with the tapes (an upper limit is also inherent to the silicones and hot-melts). The concept of compatibility also implies that the components are designed for each other, *e.g.*, a flat back surface on the j-box for tapes versus standoffs and a groove used to aid the application of silicone—which would hinder attachment and aid moisture ingress for tapes. The local topography of the module (including wires, surface roughness, and extra thickness near the j-box) may also affect adhesion.

The c-Si results also identified the dissipative behavior inherent to the foam tapes. The behavior allows the material to adjust to achieve a more stable mechanical support. In particular, this provides robustness against suddenly applied loads. The moisture present in the damp-heat test may act as a plasticizer for polymers, facilitating elongation. Also, the assembler must be careful not to stretch foam tape during its application, which may also facilitate elongation. The second acrylic tape (shown in Figure 5) is distinguished from the first acrylic tape (shown in Figure 4), which is the manufacturer's next-generation material for the j-box application.

3.3 Results of "thin film" component-level specimens

Seventeen out of forty-two c-Si j-box specimens failed the 1000 hour weight test in damp-heat. The displacement of the 4.5 kg weighted alkoxy (Ti catalyst) silicone specimen was identified between 5 and 7 days into the TF test. A representative image of the specimen is shown in Figure 6, where the displacement is identified with an arrow in the inset of the figure. No other silicone specimens demonstrated a similar appearance in the discovery experiments. From the photodocumentation of the test, it was determined that the displacement actually occurred prior to damp-heat exposure. None of the silicone specimens detached in the c-Si or TF tests (acetoxy-, alkoxy-, and oxime-cured formulations were examined in both discovery tests). The acetoxy silicone, however, did become delaminated from a glass substrate when the same set of silicones was examined in a longer-duration damp-heat test used in support of a separate project.

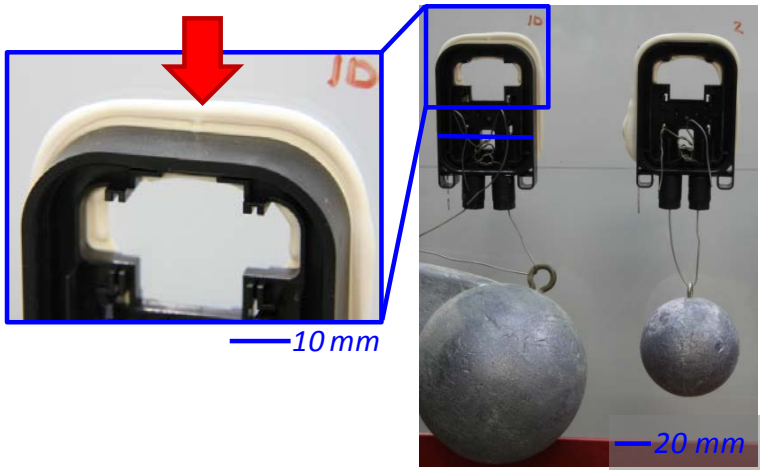

Figure 6: Images of an alkoxy (Ti catalyst) silicone (4.5 kg weight) that appeared to creep early in the test. The displacement (shown in the inset) was actually identified to have occurred before the test was started (during curing).

The displacement specimen in Figure 6 identifies the importance of the curing procedure for the silicones. The water consumed by condensation-cured silicones during curing is not abundant in steppe climate locations such as Colorado. Therefore, the manufacturer recommends a 21-day period prior to performing adhesion characterization in dry climates (whereas an adequate surface skin should be developed for use in module products within 2 days). All testing here was performed after the specimens had been allowed to cure for 21 days. The specimen in Figure 6 was

disturbed during handling after the assembly of the j-box to the substrate. Even though a cured skin had formed at the surface of the silicone, the specimen in Figure 6 was bumped prior to the 21 day storage period for curing.

The PU foam tape specimens weighted with > 0.5 kg detached within 24 hours at 85°C/85% RH. In most cases, the detachment occurred through cohesive failure of the tape's surface interface, *i.e.*, the core tape remained on the j-box while much of the surface adhesive remained on the glass. Cohesive failure of the core layer was observed for the 4.5 kg weighted specimen. The 0- and 0.5-kg weighted PU tapes remained adhered throughout the test. The 0.5 kg PU tape specimen, however, demonstrated creep of the surface adhesive layer at the adhesive/glass interface, Ref. [14]. The displaced appearance of the PU tape implies difficulty with the adhesive at the surface of the tape and not the bulk PU material. The 2.3- and 4.5-kg weighted specimens of the second acrylic tape detached within 24 hours at 85°C/85% RH. Delamination of the second acrylic tape occurred at the tape/j-box interface, *i.e.*, the tape remained on the glass. The detached acrylic tape specimens were as expected, based on the manufacturer's design guideline (maximum shear load of 1.7 kPa) [16].

The hot-melts (including the PO and PA materials) were first examined in the TF test. Representative images shown in Figure 7 depict the: (a) PO melt, (b) PA melt, and (c) PO melt. The same specimens are shown in Figure 7 (a) after 24 hours and Figure 7 (c) after 28 days. The weighted hot-melt specimens all detached within 24 hours at 85°C/85% RH. The 4.5 kg weighted PA specimen detached prior to the test. As shown in Figure 7(a), the PO specimens delaminated at the adhesive/j-box interface, *i.e.*, the melt remained on the glass. As shown in Figure 7(b), the PA specimens delaminated at the glass/adhesive interface, *i.e.*, the melt remained on the j-box. The unweighted hot-melt specimens demonstrated creep during the experiment. As shown on the right of Figure 7(c), the unweighted PO specimen displaced (until blocked by the deflector tray) relative to its original location (where the reference line scribed with a marker prior to assembly is indicated with a dashed line in the figure). Furthermore, the unweighted melt material (with no j-box attached) displaced with time [also indicated with an arrow, in the middle of Figure 7 (c), relative to the dashed line indicating the bottom edge of the j-box specimens]. Even the hot-melt lettering applied to the glass to label the specimens also demonstrated creep (translation and rotation of the asymmetric characters), indicated with an arc at the top right of Figure 7(c).

The results in Figure 7 suggest creep-facilitated detachment of the monolithic adhesive. Creep is consistent with the DSC characterization (Table 2), where melt transitions were identified to occur at temperatures less than the 85°C test temperature. The hot-melts used here were identified as potential junction box adhesives by the vendor. The results in Figure 7 are a reminder that understanding product (field) requirements (where the temperature of a module may exceed 105°C) can be critical. It should be reiterated that commercially available cross-linking hot-melt products are not expected to creep. The hot-melts examined here were used because they provided the opportunity to validate the test itself.

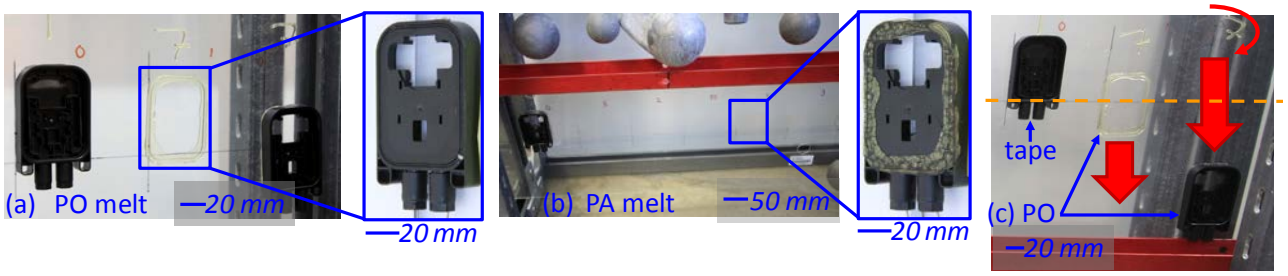

Figure 7: Images of the (a) PO and (b) PA hot-melt specimens, where detachment of the weighted specimens was observed within 24 hours at 85°C/85%RH. The details of the formerly adhered bottom-surface of the TF j-box specimens are shown in the insets. The creep of an unweighted j-box as well as the hot-melt itself are indicated in (c).

3.4 Comparison of component-level test results against material-level DMA test results

The results of DMA characterization are summarized in Figure 8 for representative materials including alkoxy (Ti catalyst) silicone, the first acrylic tape, and the PA hot-melt. The figure examines the material stiffness (shear storage modulus) and mechanical dissipation (tan [δ]) as a function of temperature. Figure 8 (conducted at 63 Hz) may be compared to a similar characterization (performed at 63 mHz) in Ref. [14]. In Figure 8, the silicone suddenly decreases in stiffness by two orders of magnitude at -34°C; however, the shear modulus remains almost unchanged above that temperature. The melt transition for the silicone is suggested from the inflection at -34°C (indicated at the bottom of Figure 8), within the relatively stable tan [δ] profile. The T_m for the silicone was -41°C in

the DSC characterization (Table 2, indicated at the top of Figure 8). The shear modulus for the acrylic tape steadily decreases by four orders of magnitude with temperature in Figure 8. (The transition in stiffness occurs over a more narrow temperature range at a slower test rate [14]). The significant mechanical damping provided by the first acrylic tape is evident in its tan [δ] profile, which is two orders of magnitude greater than that of the other materials. The maximum δ of 41.5, 33.5, 16.8, and 38.8° was observed at 63 Hz for the 1st acrylic, 2nd acrylic, PE, and PU tapes, respectively. The breadth of the tan [δ] profile for the acrylic tape is reduced with the test rate [14]. A substantial difference in the T_g for the tape occurs between the DSC characterization (at -43°C, top of Figure 8) and the DMA characterization (at 13°C, determined from the peak in the tan [δ] profile and indicated at the bottom of Figure 8). A substantial difference in the T_g for the tape occurs between the DMA conducted at 63 Hz (at 13°C, Figure 8) and the DMA conducted at 63 mHz (at -19°C, Ref. [14]). The shear modulus of the PA melt steadily decreases with temperature in Figure 8, up to 62°C. At this temperature, the test was automatically terminated when the specimen elongated by the tension supplied to the specimen to prevent it from buckling in the instrument. The T_m for the PA melt is evident in the inflection in the tan [δ] profile at 62°C. The T_g for the PA melt occurs at -57°C in DSC (Table 2), or at -2°C in DMA conducted at 63 Hz (Figure 8), or at -21°C in DMA conducted at 63 mHz [14]. The T_m for the PA melt occurs at 68°C in DSC (Table 2), or at 62°C in DMA conducted at 63 Hz (Figure 8), or at 60°C in DMA conducted at 63 mHz [14].

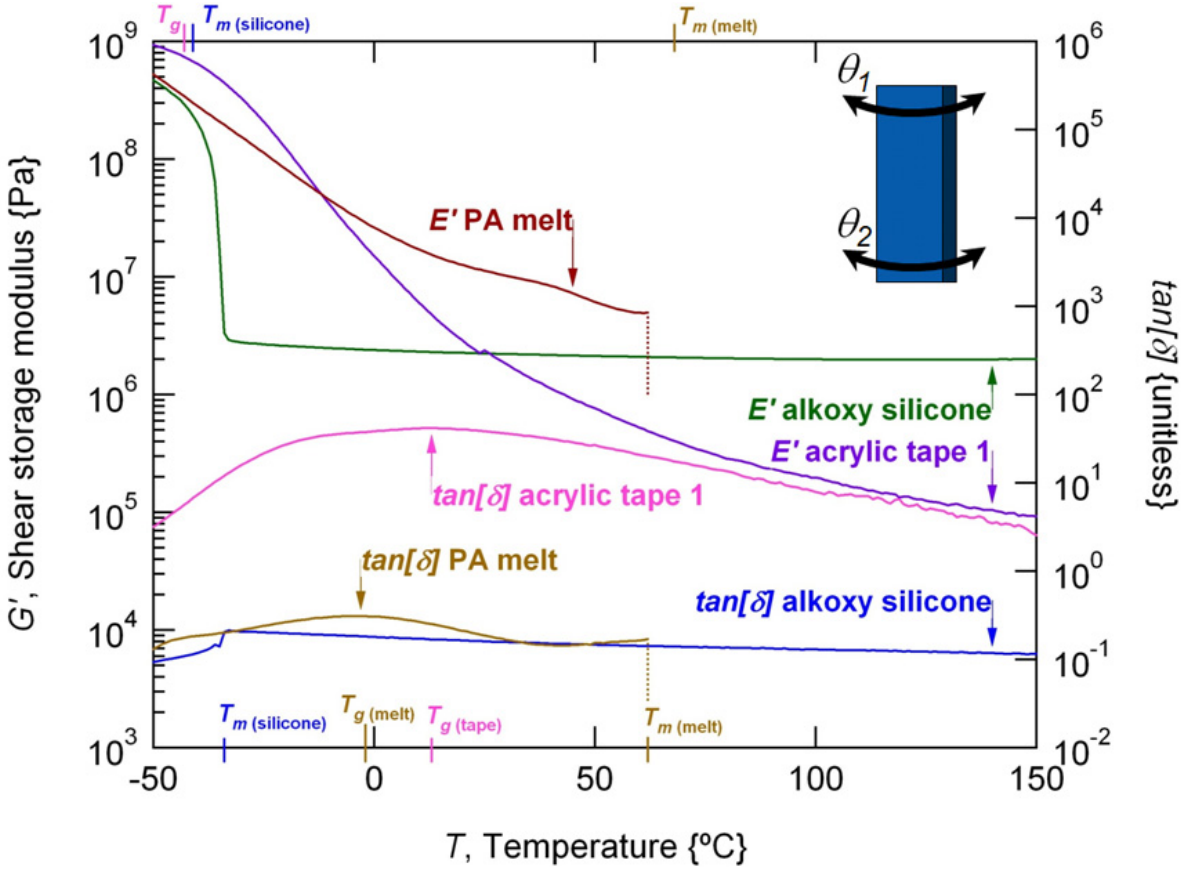

Figure 8: Summary of the torsional DMA characterization at 63 Hz for representative specimens. The phase-transitions determined from DSC are compared (figure top) to those determined using DMA (figure bottom).

Many of the results for the component-level tests can be understood from Figure 8. Furthermore, the various types of materials can be compared and contrasted using the DMA results. The sudden drop in shear modulus for the silicone at -34°C would be catastrophic if the silicone was not cross-linked (as evidenced by the stable shear modulus above that temperature). Otherwise, the silicone would be expected to demonstrate significant viscoelastic flow, as in the uncured specimen in Figure 6. The acrylic tape becomes even more compliant than the silicone at high temperature. J-boxes are, however, unlikely to be handled (*e.g.*, installed) by persons at such temperatures. Furthermore, the cables connecting a module would not ordinarily become disturbed at such temperatures in properly installed systems. All the tapes can provide significant mechanical dissipation in dynamic events such as

vibration or "impact" from wind load, which can occur at a rate on the order of tens of Hz [18]. Less dissipation is manifest in gradual loading, *e.g.*, thermal expansion (occurring at a rate on the order of 10^{-3} Hz [10], similar to Ref. [14]), or moisture swell (where strain occurs on the order of 10^{-5} to 10^{-8} Hz [19]). The minor elongation of the tape in Figure 5 over a prolonged time period may therefore be understood from its behavior at 63 mHz in Ref. [14]. It is not surprising then that the PE tape (Figure 3) and most heavily weighted PU and acrylic tapes (Figure 4) demonstrated cohesive failure (tearing often with mixed-mode failure); most tape specimens, however, did not tear but rather lost cohesion within their surface-adhesive layer. Note that some tapes have an adhesive nature throughout their thickness. The detachment and creep of the hot-melts in Figure 7 follow from their behavior shown in Figure 8. The molten thermoplastics are not able to sustain adhesion when a load (weight) is present. The molten thermoplastics creep under their own weight. Other melt products (either cross-linked or with a higher melting temperature) might work in the place of the thermoplastic hot-melts examined in Table 2.

Regarding the melt transitions, their values proved reasonably consistent with the technique (DSC vs. DMA) and the characterization rate (Figure 8 vs. Ref. [14]). That is, T_m varied less than 10°C between the DSC and DMA characterizations for the silicones and hot-melts. The glass transitions, however, were readily subject to both the technique and the characterization rate, *i.e.*, sometimes differing by more than 50°C. The T_g for the acrylic tape was the most sensitive to its rate of characterization. Although T_g, T_m, or T_f may vary by tens of degrees depending on the material composition and/or measurement technique, the values in Table 2 are generally representative for the different types of adhesives. However, a mechanical characterization at a rate of known interest (as in Figure 8) may prove a much more appropriate characterization method.

4. FUTURE WORK

The component-level discovery tests reported in this paper were preliminary to a formal component-level test. The formal test is meant to examine the proposed amendment using a representative set of known-good, known-incompatible, and intermediate ("unknown") systems. Key details of the formal test include the following:

The weights will include 0, 0.5, and 1 kg. The weights were chosen based on the multiplier (4x) recommended within the IEC working group 2. That is, the weight of 0.17 kg was obtained for two representative 1.5-m-long PV cables (with the connectors). The weight of 0.69 follows from the 4x multiplier, assuming that the self-weight of the cables constitutes the static load on a field-deployed j-box. The 0.5- and 1-kg weights bound the anticipated 0.69 kg weight; the 0 kg weight is included for reference. The formal test therefore aims to recommend either a 0.5- or 1-kg weight for the qualification tests.

Thirteen adhesives have been examined in the discovery experiments. These candidate materials have been down-selected to nine, including: the two acrylic tapes, PE tape, PU tape, acetoxy-cured silicone (Sn catalyst), oxime-cured silicone (Sn catalyst), alkoxy-cured silicone (Ti catalyst), alkoxy-cured silicone (Ti catalyst, with high green strength), and the PO hot-melt. Two types of acrylic tape will be examined to further compare the materials against the differences in Table 1 and Table 2. The adhesives for the formal test were chosen to include some known incompatible systems (prone to detaching), with many systems likely to remain attached.

The same type of junction boxes used in the discovery tests will be used in the formal test, *i.e.*, the c-Si and TF components. Four types of substrate will be used in the formal test, including: TPE [a laminate of polyvinyl fluoride (PVF), polyester, and EVA (where the PVF faces the environment)], THV [a laminate of tetrafluoroethylene, hexafluoropropylene, and vinylidene fluoride [THV], PET, and EVA (where the THV faces the environment)], KPK [a laminate of polyvinylidene fluoride [PVDF], PET, and PVDF (also Kynar, which faces the environment)], and glass (simulating a glass-glass TF module). The PVF used in backsheets typically consists of DuPont Tedlar. The backsheets to be examined, which will be adhered to a glass substrate, include the most popular types presently used in c-Si modules, which currently dominate the PV market.

The test sites for the formal test will include a subtropical location (Miami, FL), desert location (Phoenix, AZ), continental steppe climate (Golden, CO), and an indoor test chamber (the proposed damp-heat test condition). The formal test intends to verify the indoor test condition against real-world (field) environments. The weights deployed outdoors will be hung at 45° (where they will equally generate shear and tensile loads). The proposed amendment to the module qualification tests has the specimens oriented at 0° (mounted vertically; therefore, subject to a shear load only). The duration of the outdoor tests will be at least a year, whereas the indoor test is defined to last for 1000 hours.

Comparison between the outdoor and indoor results will provide important feedback. For example, the effects of cold temperature will be encountered in Golden in addition to the hot, humid environment in Miami and hot, dry environment in Phoenix. If cold weather proves significant, then a weight may be applied during the "humidity-freeze" or "thermal cycle" tests of the module qualification procedures, perhaps in addition to the damp-heat test. The comparison between specimens mounted at 45° (sometimes utilized in outdoor PV test standards) and 0° (most easily implemented in a densely packed environmental chamber) may also provide insight. The final recommendation for modification of the module qualification tests, for example, may be affected by these factors.

5. CONCLUSIONS

The early experimental work supporting a proposed amendment to the photovoltaic (PV) module qualification test standards has been described. The amendment (where a weight is added to the junction box during the damp-heat test) is intended to examine the adhesion system for the junction box (j-box). The goal of the amendment is to ensure safe and durable attachment within the early period (infant life) of field-deployed PV modules. Key results include the following:

Several key issues were identified, either from the results or based on consideration during specimen preparation. These issues include the need to:

- allow adequate time for the curing of silicone adhesives
- consider the manufacturer's design guidelines for maximum applied load (*e.g.*, the acrylic tapes)
- carefully handle foam-tape adhesives (preventing inadvertent deformation during assembly possibly enabling subsequent elongation during damp-heat)
- perform surface treatment/functionalization for some adhesives to improve interfacial attachment

Some incompatible systems were identified through the discovery tests including: acetoxy silicone/glass; polyethylene (PE) tape/polyethylene terepthalate (PET) or PE tape/glass [based on weak attachment for the adhesive layer(s)]; polyurethane (PU) tape/PET or PU tape/glass [based on weak attachment or melting of the adhesive layer(s)]; polyethylene/polyoctene copolymer (PO) or polyamide (PA) melts (and PET or glass substrates, based on creep of the adhesive).

The discovery tests also identified the usefulness of material-level characterization including thermogravimetry (TGA), differential scanning calorimetry (DSC), and dynamic mechanical analysis (DMA). For example, DSC and DMA identified the melt transition of the PO and PA thermoplastics prior to their failure in component-level testing. DMA (which may be preferred over DSC because it more directly examines mechanical behavior) also readily identified the dissipative behavior typical of the foam tapes. Comparison of the material-level and component-level tests identifies the need to understand product requirements, including the maximum operating temperature of 105°C for PV modules deployed in a desert location and the maximum local temperature during a hot-spot condition, which may exceed 150°C.

A larger formal test will follow the discovery tests described here. The formal test is intended to validate the proposed amendment using a representative set of specimens, including some known-incompatible systems and some systems expected to remain adhered. That is, the formal test will validate indoor results (the damp-heat test condition applied in a chamber) using outdoor deployed (Arizona, Colorado, Florida) specimens. Weights of 0.5 and 1 kg will be examined in the formal test, so that a final weight may be recommended for use in the qualification tests.

ACKNOWLEDGEMENTS

The authors are grateful to Dr. Peter Hacke, Dr. Michael Kempe, Dr. Heidi Pilath, Thomas Bethel, Ed Gelak, Greg Perrin, Kent Terwilliger, and David Trudell of the National Renewable Energy Laboratory for their help/discussion with indoor test chambers, material characterization, specimen fixturing, specimen handling, experimental methods, and subsequent analysis. The authors are also grateful to Mr. Scott Meyer of the 3M Company as well as Mr. Kevin Houle and Mrs. Elizabeth Kelley of the Dow Corning Corporation for help with specimen materials and the related methods. This work was supported by the U.S. Department of Energy under Contract No. DE-AC36-08GO28308 with the National Renewable Energy Laboratory.

REFERENCES

[1] R. MacDonald, M. Roosta, "Lessons Learned from Development of Silicon CPV Modules," NREL PV Module Reliability Workshop 2012.

[2] T. Sample, A. Skoczek, M.T. Field, "Assessment of Ageing Through Periodic Exposure to Damp Heat (85°/85% RH) of Seven Different Thin-Film Module Types," *Proc. IEEE PVSC* **34**, 2220–2225 (2009).

[3] W. Gambogi, S. Kurian, B. Hamzavytehrany, A. Bradley, J. Trout, "The Role of Backsheet in Photovoltaic Module Performance and Durability," *Proc. Euro PVSEC*, 3325–3328 (2011).

[4] International Electrotechnical Commission, "IEC 61215 Crystalline Silicon Terrestrial Photovoltaic (PV) Modules - Design Qualification and Type Approval," International Electrotechnical Commission: Geneva, 2005.

[5] International Electrotechnical Commission, "IEC I61646 Thin-Film Terrestrial Photovoltaic (PV) Modules – Design Qualification and Type Approval," International Electrotechnical Commission: Geneva, 2008.

[6] International Electrotechnical Commission, "IEC 60068-2-21 Environmental Testing Part 2-21: Tests – Test U: Robustness of Terminations and Integral Mounting Devices," International Electrotechnical Commission: Geneva, 2006.

[7] European Committee for Electrotechnical Standardization, "EN 50548: Junction Boxes for Photovoltaic Modules," European Committee for Electrotechnical Standardization: Brussels, 2012.

[8] D.L. King, W.E. Boyson, J.A. Kratochvil, "Photovoltaic Array Performance Model," SAND2004-3535, 1–43, (2004).

[9] D. Faiman, "Assessing the Outdoor Operating Temperature of Photovoltaic Modules," *Prog. Photovolt: Res. Appl*. **16**, 307–315 (2008).

[10] D.C. Miller, M.D. Kempe, S.H. Glick, S.R. Kurtz, "Creep in Photovoltaic Modules: Examining the Stability of Polymeric Materials and Components," *Proc. IEEE PVSC* **35**, 262–268 (2010).

[11] E. Molenbroek, D.W. Waddington, K.A. Emery, "Hot Spot Susceptibility and Testing of PV Modules," *Proc. IEEE PVSC* **22**, 547–552 (1991).

[12] J. Oh, G. Tamizhmani, "Temperature Testing and Analysis of PV Modules per ANSI/UL 1703 and IEC 61730 Standards," *Proc. IEEE PVSC* **35**, 984–988 (2010).

[13] M.D. Kempe, S.R. Kurtz, J.H. Wohlgemuth, D.C. Miller, M.O. Reese, A.A. Dameron, "Modeling of Damp Heat Testing Relative to Outdoor Exposure,", Proc Asian PVSEC 2011.

[14] D.C. Miller, J.H. Wohlgemuth, S.R. Kurtz, "A Proposed Junction-Box Stress Test (Using an Added Weight) for Use During the Module Qualification," NREL PR-5200-54525, (2012). (http://www.nrel.gov/docs/fy12osti/54525.pdf, the presentation from this conference will also issue as a more current NREL "report")

[15] D.C. Miller, M.T. Muller, M.D. Kempe, K. Araki, C.E. Kennedy, S.R. Kurtz, "Durability of Polymeric Encapsulation Materials for Concentrating Photovoltaic Systems", *Prog. Photovolt: Res. Appl*. (DOI: 10.1002/pip.1241)

[16] T. Kremer, "Useful Design Criteria for Acrylic Foam Tapes in Demanding Industrial Applications", Proc. Pressure Sensitive Tape Council (PSTC), (2005).

[17] M. Noeske, J. Degenhardt, S. Strudthoff, U. Lommatzsch, "Plasma Jet Treatment of Five Polymers at Atmospheric Pressure: Surface Modifications and the Relevance for Adhesion," *Intl. J. Adhesion Adhesives* **24**, 171–177 (2004).

[18] K.-A. Weiss, M. Assmus, S. Jack, K. Köhl, "Measurement and Simulation of Dynamic Mechanical Loads on PV-Modules," *Proc. SPIE* **7412**, 741203 (2009).

[19] M.D. Kempe, "Modeling Rates of Moisture Ingress into Photovoltaic Modules," *Solar Energy Mats. Solar Cells* **90**, 2720–2738 (2006).